International Journal of Applied Pharmaceutics

ISSN- 0975-7058 Vol 17, Issue 1, 2025

Original Article

SILK FIBROIN-COATED MESOPOROUS SILICA NANOPARTICLES ENHANCE 6-THIOGUANINE DELIVERY AND CYTOTOXICITY IN BREAST CANCER CELLS

MOHAMMAD AMIN KABOLI[1,2], ALAA A. HASHIM[3], DHIYA ALTEMEMY[4], JAVAD SAFFARI CHALESHTORI[5], MEHDI REZAEE[2], SAYEDEH AZIMEH HOSSEINI[2], PEGAH KHOSRAVIAN[6*]

[1]Student Research Committee, Shahrekord University of Medical Sciences, Shahrekord, Iran. [2]Department of Medical Biotechnology, School of Advanced Technologies, Shahrekord University of Medical Sciences, Shahrekord, Iran. [3]Department of Pharmaceutics, College of Pharmacy, Ahl AL-Bayt University, Karbala, Iraq. [4]Department of Pharmaceutics, College of Pharmacy, Al-Zahraa University for Women, Karbala, Iraq. [5]Clinical Biochemistry Research Center, Basic Health Sciences Institute, Shahrekord University of Medical Sciences, Shahrekord, Iran. [6]Medical Plants Research Center, Basic Health Sciences Institute, Shahrekord University of Medical Sciences, Shahrekord, Iran

[*]Corresponding author: Pegah Khosravian; [*]Email: pegah.khosraviyan@gmail.com

Received: 07 Oct 2024, Revised and Accepted: 07 Dec 2024

ABSTRACT

Objective: Breast cancer stands as the most prevalent form of cancer among women globally. Conventional chemotherapy, including the use of 6-Thioguanine (TG), often faces limitations such as poor drug solubility. In this research, we engineered a nanosystem consisting of Mesoporous Silica Nanoparticles (MSNs) loaded with TG and coated with Silk Fibroin (SF) to enhance the pharmacokinetic properties of this drug in targeting the MCF-7 breast cancer cell line.

Methods: In this study, we investigated the cytotoxicity of different formulations through MTT assay. Additionally, we analyze apoptosis and cell cycle phase distribution using flow cytometry. Furthermore, the absorption of MSN nanoparticles by MCF-7 cells was investigated using the fluorescent labeling technique by Dil fluorochrome.

Results: Our results represented the 48 h Half Maximal Inhibitory Concentration (IC_{50}) values of free TG, MSNs loaded with TG (TG@MSNs) and SF-coated MSNs loaded with TG (SF/TG@MSN) were 16.69, 10.96 and 8.01 µM, respectively. Moreover, the percentage of total early and late apoptosis differed among the treatments. Specifically, cells treated with free TG, TG@MSN and SF/TG@MSN exhibited 13.49%, 76.05% and 84.99% apoptosis, respectively. The results also indicated that administering free TG and TG-loaded MSN nanoparticles to MCF-7 cells resulted in cell cycle arrest at the G2/M phase after 48 h of treatment.

Conclusion: Our study demonstrated that the SF/TG@MSN nanosystems effectively increased the cytotoxic effects of TG on the breast cancer cell line.

Keywords: 6-Thioguanine, Apoptosis, Breast adenocarcinoma, Cell cycle, Mesoporous silica nanoparticles (MSNs)

DOI: https://dx.doi.org/10.22159/ijap.2025v17i1.52882 Journal homepage: https://innovareacademics.in/journals/index.php/ijap

INTRODUCTION

Breast cancer can have terrible consequences and affects more women globally than any other type of disease. Unbelievably, 685,000 women lost their lives to breast cancer in 2020 and 2.3 million women received a diagnosis [1, 2]. As a leading cause of cancer-related mortality in Iran, it ranks first among female cancers and accounts for 21.4% of all cancer cases [3, 4]. While advancements in surgery, chemotherapy, radiation therapy and targeted treatments have improved survival rates, challenges persist, particularly in cases of metastatic and treatment-resistant breast cancer [5, 6]. Conventional chemotherapy, including the use of TG, often faces limitations such as poor drug solubility, rapid clearance, lack of selectivity towards cancer cells and severe side effects [7]. These limitations can lead to suboptimal therapeutic outcomes and significant toxicity for patients. To combat the devastating impact of breast cancer, scientists are exploring innovative solutions, such as nanotechnology-based drug delivery systems. This promising approach aims to improve the effectiveness and safety of anticancer treatments [8]. Nanotechnology can overcome these limitations by improving drug solubility, enhancing targeted delivery to tumor sites and reducing systemic toxicity [9]. With their high surface area, readily functionalized surface, biocompatibility and varying pore size, MSNs have become a valuable platform in drug delivery research. Due to their unique properties, MSNs are well-suited for encapsulating and transporting medicinal substances [10, 11]. These characteristics empower MSNs to effectively encapsulate hydrophobic drugs like TG, enhancing their absorption into cells and potentially circumventing multidrug resistance in cancer [12]. MSNs are used in targeted drug delivery devices because they are biocompatible, have low toxicity and can hold a large dose of the drug. Each of these nanoparticles can hold between 200 and 300 mg of the drug, with a maximum of about 600 mg per 1 g of silica [13]. Thioguanine, a purine analog antimetabolite, has shown promise in treating various cancers, including acute and chronic myeloid leukemia, inflammatory bowel disease and potentially triple-negative breast cancer [14, 15]. By interfering with the PI3K-AKT pathway, an essential signaling route for cancer cell survival and proliferation, it promotes apoptosis and inhibits cell proliferation, thereby exhibiting anticancer actions [16]. However, a significant hurdle lies in TG's low solubility in water, hindering its bioavailability and necessitating higher doses to achieve therapeutic effects.

Thiopurine treatments, including TG, are also known to cause dose-dependent side effects like myelotoxicity, skin rash, hair loss, joint pain, nausea, flu-like symptoms and diarrhea. High doses can even lead to kidney failure [17]. Although current TG treatments have limitations, research suggests that TG's mode of action, which involves causing arrest of cell cycle and demise in cancer cells through DNA mismatch, offers a promising direction for further investigation in developing efficient breast cancer therapies [18, 19]. In recent decades, silk has gained prominence in the medical field. Silk threads, comprising fibroin and sericin protein fibers [20], offer unique advantages. The advantageous qualities of SF, including cell adhesion, biodegradability, biocompatibility and minimal immunological response, lead to its excellent application in tissue development and regenerative therapies [21]. Research indicates that nanocarriers can enhance TG medication delivery to tumor tissue.

Consequently, this leads to a higher effectiveness in inhibiting cancer growth in breast cancer cells while using a smaller drug dose [22, 23]. Furthermore, SF as a coating for nanocarriers can improve cellular uptake, thereby enhancing the antitumor properties of

nanosystems [24, 25]. Due to its unique properties, SF has garnered significant attention in drug delivery applications. The amphiphilic properties of SF, characterized by its hydrophobic crystalline domains and hydrophilic amorphous regions, enable it to interact with the surface of nanoparticles and the cell membrane [26]. Recent advancements in nanocarrier designs also support this approach, emphasizing the importance of surface modification for improved cellular uptake [27]. Combining MSNs, TG and SF coating may be an innovative strategy to treat breast cancer. This synergistic combination aims to leverage the high loading capacity of MSNs, TG's anticancer properties and SF's biocompatibility and cellular uptake-enhancing potential. We hypothesize that this SF/TG@MSN system will improve TG's pharmacokinetic profile and enhance its cellular uptake and cytotoxic effects against breast cancer cells.

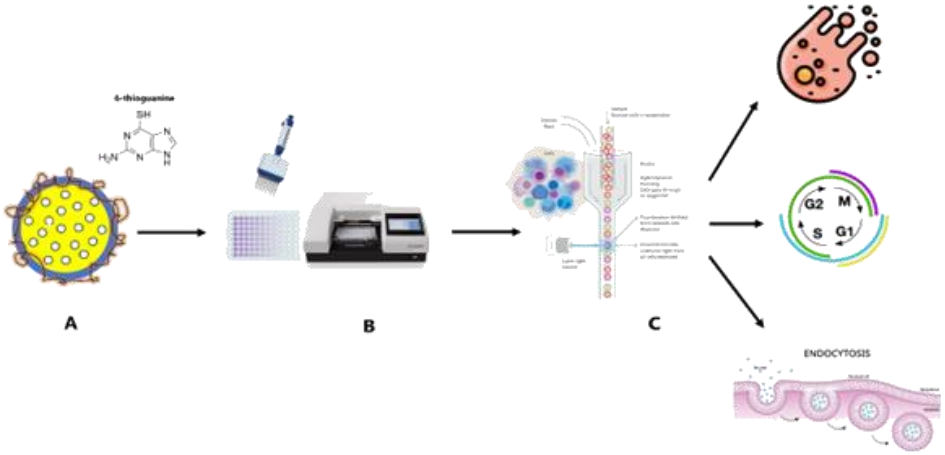

Fig. 1: Schematic illustration of study design. (a) 6-TG loaded mesoporous silica nanoparticle coated with SF. (b) Cytotoxicity was evaluated using an MTT assay and formazan absorbance was measured at 570/630 nm. (c) flow cytometric assessment of apoptosis, cell cycle phase distribution and cellular uptake of nanoparticles

MATERIALS AND METHODS

Materials

This study utilized the following materials: MTT (3-(4,5-Dimethylthiazol-2-Yl)-2,5-Diphenyltetrazolium Bromide), trypan blue, propidium iodide, Dil (3′-tetramethyl indocarbocyanine perchlorate) and ribonuclease A (Sigma-Aldrich Chemical Co. Ltd) 6-thioguanine and Dimethyl Sulfoxide (DMSO) (Merck, Darmstadt, Germany) Dulbecco's Modified Eagle's Medium (DMEM) with high glucose, trypsin EDTA, Fetal Bovine Serum (FBS), Penicillin-Streptomycin (10,000 U/ml) and Phosphate-Buffered Saline (PBS) (Idea Zist Recombinant Company, Iran) MCF-7 cell line (Pasteur Institute of Iran) FITC Annexin V Apoptosis Detection Kit with PI (Padza Padtan Pajooh Co).

Characteristics of nanoparticles

The method described by Altememy *et al.* (2020) [28] was followed for synthesizing the nanoparticles in their study on SF-coated MSNs for targeted TG delivery in leukemia. The MSNs were produced using a sol-gel method with Cetrimonium Bromide (CTAB) as a cationic surfactant template. The resulting MSN nanoparticles had an approximate size of 100 nm and a pore diameter of 3.2 nm.

The TG Loading Efficiency (LE) and Loading Capacity (LC) were determined to be 51.04% and 33.79%, respectively, for TG@MSN and 18.75% and 14.45% for SF/TG@MSN. Dynamic Light Scattering (DLS) analysis revealed zeta potentials of-25,-28 and-20.65 for MSN, TG@MSN and SF/TG@MSN, respectively.

Cell culture

MCF-7 cells were cultured in a high-glucose Dulbecco's Modified Eagle's Medium (DMEM) supplemented with L-glutamine (4 mmol), 10% heat-inactivated FBS and 1% penicillin-streptomycin (10,000 U/ml). The cells were cultured in a controlled environment at 37 °C, with a humidity level of 95% and a carbon dioxide concentration of 5%. The adherent cells were separated using a 0.25% trypsin-EDTA solution and the cell viability was determined using a Neubauer Hemocytometer and the trypan blue exclusion method [29, 30].

In vitro cytotoxicity assay

The MTT assay assessed the cytotoxic effects of free TG, TG@MSNs, SF/TG@MSN, MSNs and MSNs@SF on MCF-7 cells. The cells were seeded at 10,000 per well in 96-well Microplates and treated under CO_2 for 24 h. TG, TG-MSNs and TG-MSNs@SF were added at various concentrations (5, 10, 20, 40, 80, 100 and 200 µM) and incubated for 48 h. After that, MTT (5 mg/ml) was applied to the treated and vehicle control cells (with 1% DMSO) and incubated at 37 °C for 3 h.

After removing MTT, DMSO was used to dissolve the insoluble formazan crystals formed by mitochondrial reductase enzymes in live cells. The plates were gently shaken for 15 min and then cell viability was measured by reading the plates at 570 nm on a microplate reader (Stat fax-2100 Awareness Technology, Inc.). The IC_{50} of free TG, TG@MSNs and SF/TG@MSN, which reduce cell growth by 50%, were calculated using dose-response curves. Cell viability was graphed as TG, TG-MSN and TG-MSN@SF concentrations increased [31, 32]. To determine the IC_{50} values, a nonlinear regression equation was used:

$$\text{Cell viability (\%)} = \frac{\text{OD570}-630\ \text{treatment}}{\text{OD570}-630\ \text{control}} \times 100$$

Apoptosis assay

Cell apoptosis was assessed using the annexin V-FITC/PI assay and a CyFlow™ Space-Sysmex flow cytometer. MCF-7 cells were seeded at 3x105/well and grown at 37 °C in 5% CO_2 for 24 h. For 48 h, cells were treated with free TG, TG@MSNs, SF/TG@MSN, MSNs and MSNs@SF at their IC_{50} concentrations. We suspended the cells in 100 µl of 1X annexin V binding buffer at 10^6 cells/ml following treatment and washing with the same buffer. Annexin V-FITC solution (1 µl) was added, followed by a 15-minute dark incubation at room temperature. After adding one µl of PI solution to each sample, the mixture was incubated for 5 min in dark conditions. After centrifugation at 300 g for 10 min, the cells were washed with 1X PBS and resuspended in 400 µl for flow cytometry analysis [33, 34].

Cell cycle distribution analysis

They incubated 3×10^5 MCF-7 cells per well in a 6-well plate for 24 h to assess cell cycle distribution. For 48 h, the cells were treated with free TG, TG@MSNs, SF/TG@MSN, MSNs and MSNs@SF at their IC_{50} concentrations. After treatment, cells were washed, trypsinized and fixed in cold ethanol. After fixation, the cells were rinsed again, treated with RNase A and stained with propidium iodide. Then, flow cytometry with the FL2 channel and ModFit LT version 5 was used to determine cell cycle stage distribution [33].

In vitro cellular uptake

Dil (1,1'-dioctadecyl-3,3,3',3'-tetramethylindocarbocyanine perchlorate) fluorescent labeling was used to determine whether MCF-7 cells internalize MSNs. Dil (1 mg/ml, 100 µl) dissolved in ethanol was combined with 20 mg of calcinated MSN, subjected to continuous agitation in darkness for 24 h and subsequently centrifuged. The resulting precipitate was subjected to multiple ethanol washes to eliminate unbound dye, followed by a 24-hour freeze-drying process to yield Dil@MSN as a dry powder. The synthesis of SF/Dil@MSN nanoparticles followed a similar protocol, adding 1 ml of fibroin solution (2.2 mg/ml in DMSO) post-Dil loading.

For the cellular uptake assay, MCF-7 cells ($3x10^5$ cells/well) were seeded into a 6-well plate and allowed to adhere for 24 h. Dil@MSN and SF/Dil@MSN nanoparticle suspensions (100 µg/ml) were introduced into the wells and the plates were incubated at 37 °C for 48 h. Flow cytometry was used with the FL2 channel to quantify the mean fluorescence intensity of Dil within the cells. Results were analyzed using FlowJo™ software version 7.6 [33].

Statistical analysis

Each experiment was repeated three times using GraphPad Prism 8. A one-way analysis of variance (ANOVA) was used to determine treatment group statistical differences in the treatment group. The mean±SD is displayed for each result. Statistical significance was determined at $p<0.05$ and post-hoc analyses were conducted to differentiate groups [35].

RESULTS

In vitro cytotoxicity assay

The MTT assay demonstrated a dose-dependent cytotoxic effect of free TG, TG@MSNs and SF/TG@MSN on MCF-7 cells, with cell viability decreasing significantly as concentrations increased from 5 to 200 µM (fig. 1A). In contrast, MSNs and SF@MSNs did not exhibit significant cytotoxicity and were considered non-toxic to MCF-7 cells (fig. 1B). According to table 1, the IC_{50} values following 48 h of treatment for free TG, TG@MSNs and SF/TG@MSN were 16.69 µM, 10.96 µM and 8.01 µM, respectively. These findings suggest that MSN nanoparticles enhanced the cytotoxic effect of TG on MCF-7 cells, with the IC_{50} value of SF/TG@MSN being approximately half that of free TG.

Table 1: IC_{50} values (48 h) of free TG, TG@MSN and SF/TG@MSN

Treatment	IC_{50} (µM)
Free TG	16.69±0.25
TG@MSN	10.96±0.15
SF/TG@MSN	8.01±0.12

Results are expressed as the mean±standard deviation (n = 3).

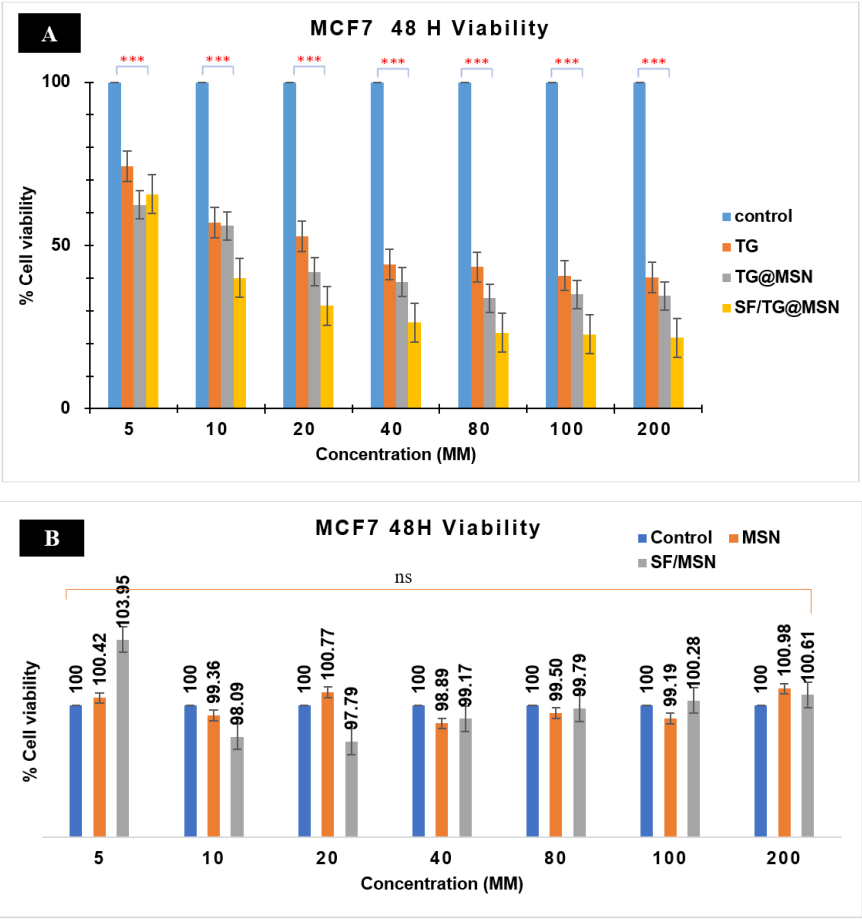

Fig. 2: A histogram illustrates the dose-dependent cytotoxic effects of (a) free TG, TG@MSNs and SF/TG@MSN, as well as (b) MSNs and SF@MSNs on MCF-7 cells compare to control group. The results are expressed as mean±SD. Statistical significance is denoted by ns for no significance (p-value>0.05) and * for p<0.001**

Apoptosis assay

The apoptotic effect of various formulations, such as free TG and MSN nanoparticles, was assessed using annexin V/FITC and PI staining (fig. 2). The analysis demonstrated varying percentages of total early and late apoptosis among treatments. Specifically, cells treated with free TG, TG@MSN and SF/TG@MSN exhibited 13.49%, 76.05% and 84.99% apoptosis, respectively (table 2). Unlike the control group, MSN and SF@MSN formulations showed no significant apoptosis, supporting the cytotoxicity assay results for these nanoparticles.

The apoptosis assay revealed that TG@MSN and SF/TG@MSN induced apoptosis at rates significantly higher (approximately 5.63-fold and 6.3-fold, respectively) than free TG. These findings suggest that the MSN nanoparticle delivery system substantially improves the pharmacokinetics of TG, resulting in greater therapeutic efficacy. Additionally, the use of SF as a coating agent in the delivery system further demonstrates its potential to enhance the efficacy of the treatment against MCF-7 cells.

Table 2: Distribution of normal cells, early and late apoptosis and necrotic cells following 48 h of treatment

Group	Normal cell	Early apoptosis	Late apoptosis	Necrosis
Control	99.14±0.33	0.35±0.07[a]	0.17±0.04	0.075±0.03
Free TG	87.58±1.65	9.62±2.28[b]	2.65±0.67	0.13±0.06
TG@MSN	23.56±0.43	73.37±0.04[c]	3.01±.43	0.04±0.04
SF/TG@MSN	11.93±4.30	81.66±5.11[d]	6.37±0.81	0.03±0.02
MSN	94.64±2.75	2.54±0.57[a]	2.15±1.71	0.2±0.15
SF@MSN	93.22±2.34	3.1±0.55[a]	3.42±1.93	0.27±0.17

Value are reported as mean±SD (n=3). Significant differences are observed between values in columns marked by various superscripts ($p<0.05$).

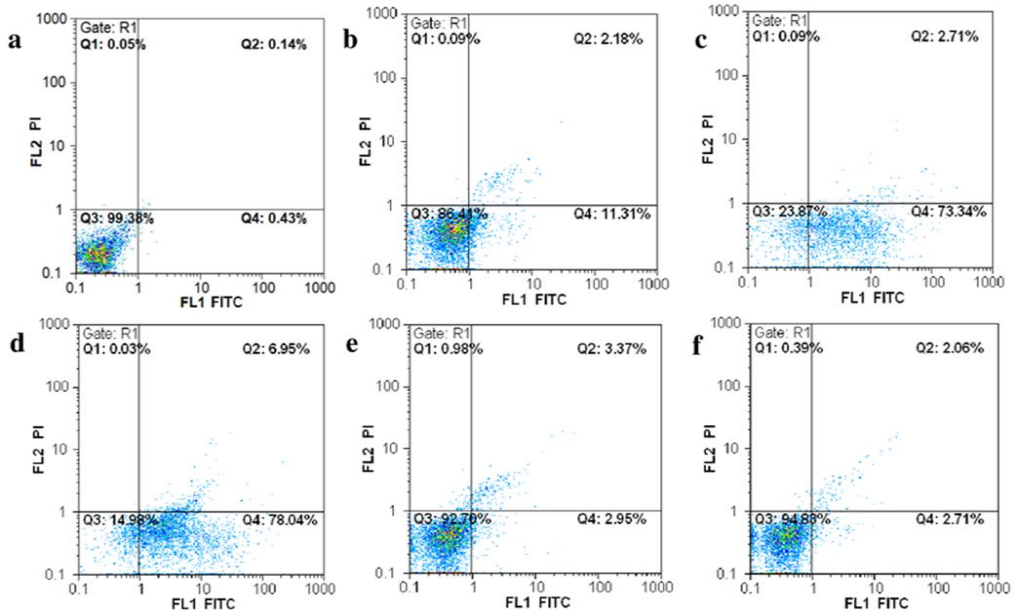

Fig. 3: Quadrant representation of flow cytometry analysis of apoptosis in MCF-7 cells following the application of annexin V-FITC/PI staining: (a) Control, (b) free TG, (c) TG@MSN, (d) SF/TG@MSN, (e) MSN and (f) SF@MSN

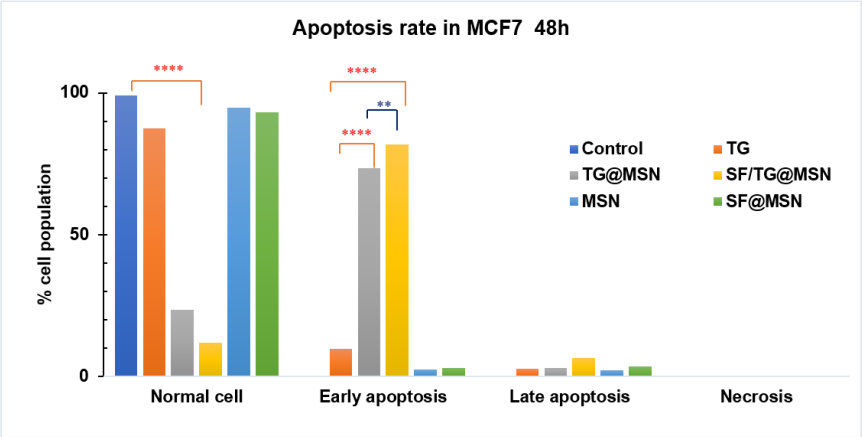

Fig. 4: A histogram representation of cell population percentage in a different stage of apoptosis and necrosis after 48 h of treatment with free TG, TG@MSN, SF/TG@MSN, MSN and SF@MSN, value are mean±SD (**p<0.0001, **p<0.01)**

Cell cycle analysis

Cell cycle analysis using flow cytometry was conducted to assess the inhibitory effect of TG on the proliferation of MCF-7 cells. Free TG and nanoparticle formulations affected cell cycle distribution, as seen in fig. 4 and 5. Free TG, TG@MSN and SF/TG@MSN increased the G2/M phase cell population compared to the control group. Table 3 shows the cell age distribution in each cell cycle phase

(mean±SD, n=3), with G2/M populations of 5.02±0.73, 18.99±0.26, 28.2±3.18 and 39.11±3.24 for control, free TG, TG@MSN and SF/TG@MSN groups, respectively.

These findings indicate that treatment with free TG and TG-loaded MSN nanoparticles caused MCF-7 cells to enter a cell cycle arrest at the G2/M phase following 48 h. This arrest is likely attributable to Mismatch Repair (MMR) pathway activation, which activates ATM-Chk2 and ATR-Chk1 protein kinases. These kinases, in turn, increase p21 protein activity and inhibit the CDK1/cyclin B complex, culminating in G2/M phase arrest.

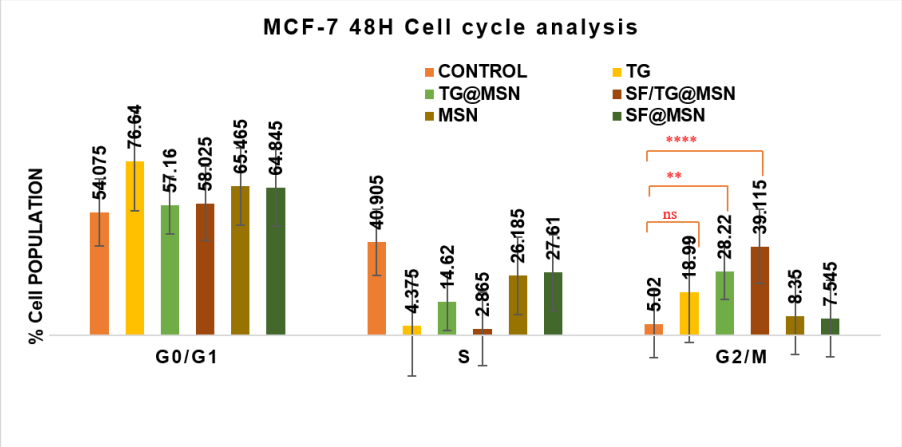

Fig. 5: A histogram showing the percentage of cells in different stages of the cell cycle after being treated for 48 h with free TG, TG@MSN, SF/TG@MSN, MSN and SF@MSN, value are mean±SD and ****p<0.0001 and **p<0.01

The increased G2/M arrest seen with SF/TG@MSN treatment suggests that the SF/MSN system amplifies TG's impact on the cell cycle. This enhanced effect is likely attributed to improved nuclear delivery of TG, which results in more widespread DNA damage and the subsequent triggering of cell cycle checkpoints [36].

Table 3: Parts of the MCF-7 cell population in each stage of the cell cycle after 48 h of treatment

Phase	Control (%)	Free TG (%)	TG@MSN (%)	SF/TG@MSN (%)	MSN (%)	SF@MSN (%)
G0/G1	54.1±2.69	76.64±0.11	57.16±0.82	58.02±2.49	65.46±6.51	64.84±10.47
S	40.9±1.95	4.37±0.16	14.62±4	2.86±0.74	26.18±6.32	27.61±15.92
G2/M	5.02±0.73	18.99±0.26	28.2±3.18	39.11±3.24	8.35±0.18	7.54±5.45

Results are expressed as the mean±standard deviation (n = 3).

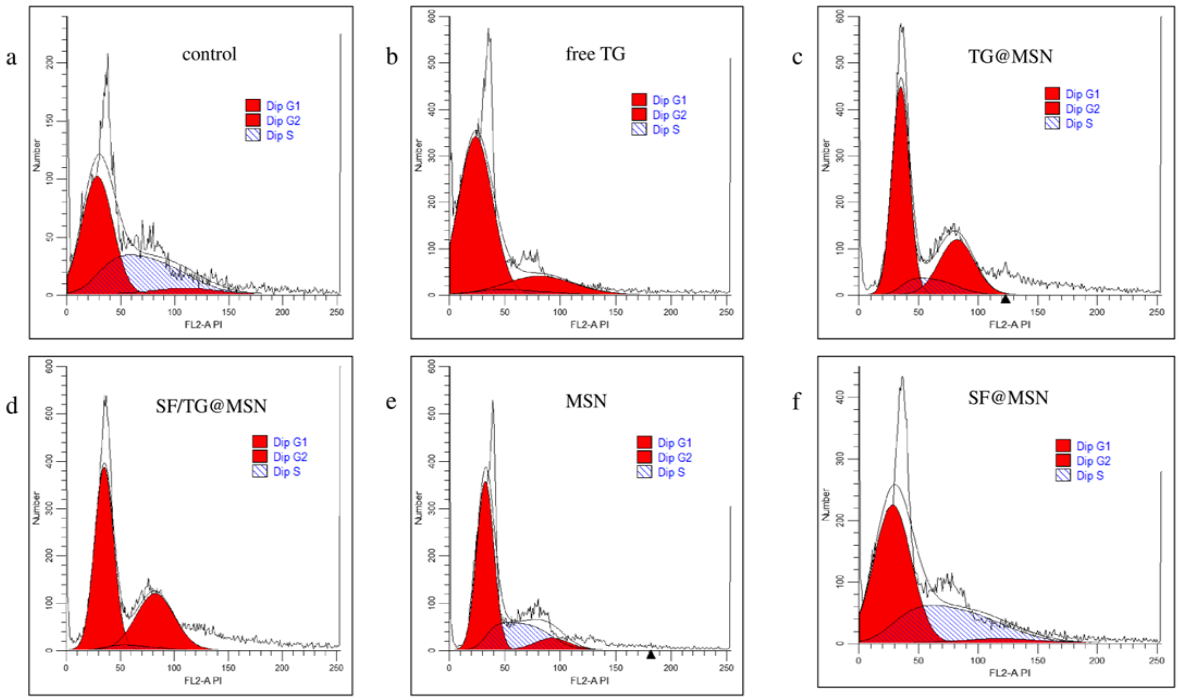

Fig. 6: PI/RNase tagging was used to look at the MCF-7 cell cycle distribution using flow cytometry. The following categories are included: (a) Control, (b) free TG, (c) TG@MSN, (d) SF/TG@MSN, (e) MSN and (f) SF@MSN

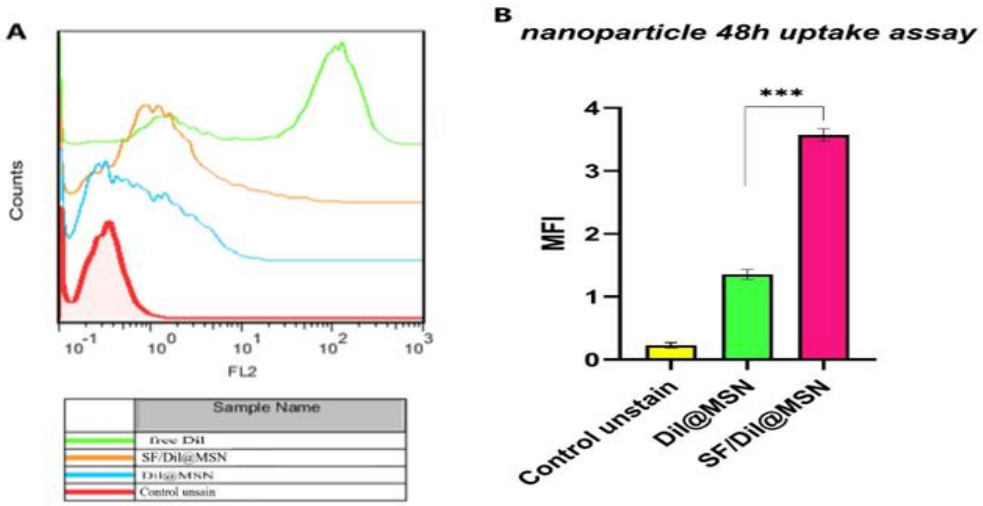

Fig. 7: Quantification of cellular uptake of different nanoparticle formulations after 48 h of exposure. (a) Fluorescence intensity of Dil@MSN and SF/Dil@MSN compared to control groups. (b) MFI values of Dil@MSN and SF/Dil@MSN, Value are mean±SD (*p<0.001)**

***In vitro* cellular uptake**

The cellular uptake of different nanoparticle formulations was assessed *in vitro* by measuring the emission intensity of fluorescent-labeled nanoparticles in the FL2 channel. Fig. 6A shows that the unstained control group had negligible fluorescence, confirming no autofluorescence. Notably, cells treated with SF/Dil@MSN exhibited higher intensity than those treated with Dil@MSN, suggesting that SF/MSN nanoparticles labeled with DiI were taken up more efficiently by the MCF-7 breast cancer cells. These findings are consistent with the results of the cytotoxicity and apoptosis assays.

Quantitative analysis in (fig. 6B) further supports this. The mean fluorescence intensity (MFI) was significantly higher in the SF/Dil@MSN group compared to Dil@MSN (3.57±0.09 vs. 1.35±0.07), indicating more effective uptake of SF/MSN nanoparticles. Interestingly, cells treated with free Dil showed the highest fluorescent intensity, suggesting greater uptake or accumulation. The higher fluorescence intensity of free Dil may be due to its lipophilic nature, which allows it to readily integrate into cell membranes.

DISCUSSION

Ongoing research and development of more efficacious medicines for breast cancer is imperative due to its status as the leading cause of mortality among women [37], constituting 21.4% of all cancer cases in Iran. Recent research has focused on enhancing drug delivery systems to improve medication efficacy [38-42]. This study investigated the therapeutic impact of SF-coated MSNs containing TG on MCF-7 breast cancer cells, focusing on their anticancer properties. Cytotoxicity tests revealed that the 48-hour IC_{50} values (concentrations causing a 50% reduction in cell growth) for free TG, TG@MSN and SF/TG@MSN were 16.69, 10.96 and 8.01 µM, respectively, underscoring the superior efficacy of the fibroin-coated nanoparticle system in delivering TG to MCF-7 breast cancer cells. Based on these findings, it appears that encapsulating TG with SF and loading it into MSNs increases the cellular toxicity of the medication in breast cancer cells. The finding that encapsulation increases toxicity is supported by Bhavsar *et al.* (2020) [43], who showed that doxorubicin-loaded chitosan folate-capped MSNs were more hazardous to MCF-7 and MDA-MB-231 cells than either free doxorubicin or doxorubicin-MSN. Additionally, Aghevlian *et al.* (2013) [44] discovered that in MCF-7 cells, TG-loaded gold nanoparticles had a more decisive antiproliferative action compared to free TG, also found that TG-loaded gold nanoparticles exhibited higher antiproliferative activity than free TG in MCF-7 cells.

Apoptosis tests demonstrated that combining MSNs and SF coating significantly enhances apoptosis induction in MCF-7 cells. The percentage of cells undergoing early and late apoptosis increased from 13.49% with free TG to 84.99% with SF/TG@MSN. This observation aligns with the findings of Deka *et al.* (2023), who reported a substantial increase in apoptotic signals in HeLa cells treated with hyaluronic-dodecyl amide conjugate nanoparticles loaded with TG [45].

The study further revealed that free TG and TG-loaded nanoparticles (TG@MSN and SF/TG@MSN) induce G2/M cell cycle arrest in MCF-7 cells. This observation is consistent with prior research demonstrating TG's ability to trigger G2/M arrest [23, 46]. The enhanced cytotoxicity and apoptosis in TG@MSN and SF/TG@MSN groups are likely due to increased TG delivery to cancer cells facilitated by these nanosystems.

The SF/TG@MSN system's improved efficacy is attributed to several factors. The amphiphilic nature of SF enhances cellular uptake [47] and specific amino acid sequences like RGD (Arg-Gly-Asp) promote binding to cell surface integrins. The pH-responsive behavior of SF may also facilitate endosomal escape, releasing TG into the cytoplasm [48]. This efficient intracellular delivery could explain the enhanced cytotoxicity and apoptosis induction observed with SF/TG@MSN compared to free TG.

The increased apoptosis and G2/M arrest reported with SF/TG@MSN therapy may have multiple molecular causes. TG, a purine analog, damages DNA during replication and activates the DDR (DNA Damage Response) pathway [49]. The increased delivery of TG to the nucleus via the SF/MSN system may cause more extensive DNA damage, overwhelming the cell's repair mechanisms. This mechanism aligns with findings from recent studies that highlight the role of enhanced drug delivery systems in augmenting DNA damage and apoptosis in cancer cells [50].

ATM/ATR kinases phosphorylate downstream effectors such as Chk1 and Chk2 to activate the DDR pathway [36]. These effectors, in turn, can activate p53, leading to the upregulation of pro-apoptotic proteins like Bax (BCL2 Associated X, Apoptosis Regulator) and PUMA (p53 Upregulated Modulator of Apoptosis). Simultaneously, p53 can induce p21, a cyclin-dependent kinase inhibitor that promotes G2/M arrest by inhibiting the Cdc2/Cyclin B complex. The strong G2/M arrest observed with SF/TG@MSN therapy suggests strong cell cycle checkpoint activation. This arrest gives cells time to repair DNA damage or apoptosis if it is too significant. The study's large percentage of apoptotic cells suggests that many cells cannot overcome TG-induced damage due to the SF/MSN system's persistent and higher TG levels.

SF/TG@MSN's increased apoptosis may be due to the mitochondrial pathway. TG-induced DNA damage releases mitochondrial cytochrome c, activating caspase-9 and caspase-3, causing apoptosis [49]. Effective TG administration by SF/TG@MSN may enhance this cascade, contributing to this study's elevated apoptosis. The finding

shows SF/TG@MSN can induce mitochondrial apoptosis in breast cancer cells.

This study, while insightful, has limitations. An *in vitro* model is insufficient to replicate human breast cancer complexity. Studies are needed to evaluate the pharmacokinetics, biodistribution and potential toxicity *in vivo* [51, 52]. Additionally, the study did not account for variability between breast cancer subtypes [53].

Despite limitations, SF/TG@MSN shows promise as a therapeutic strategy. However, the clinical application requires comprehensive preclinical studies, safety and efficacy evaluations [54, 55], regulatory approval [56], clinical trials [57] and scalable manufacturing processes [58]. Recent reviews have outlined the critical steps in translating nanomedicine from bench to bedside, highlighting the challenges and strategies for successful clinical adoption [59].

CONCLUSION

This study examines the toxic effects of silk fibroin-coated mesoporous silica nanoparticles containing thioguanine compared to free thioguanine while targeting the MCF-7 breast cancer cell line in a laboratory setting. The findings indicated that the SF/TG@MSN nanosystems significantly increased the toxicity of TG against this particular breast cancer cell line. Furthermore, the administration of free TG resulted in cell cycle arrest, specifically at the G2/M phase. This arrest was significantly more significant in the TG@MSN and SF/TG@MSN groups. Additional *in vitro* research on breast cancer cell lines, such as MDA-MB-231, is recommended to thoroughly assess the anticancer characteristics of SF/TG@MSN. Furthermore, *in vivo* experiments are essential to authenticate these discoveries and bolster the clinical use of this nano-drug. The results of this research are crucial to furthering the practical application of SF/TG@MSN in breast cancer treatment.

ACKNOWLEDGMENT

Project 6630 and ethical code IR. SKUMS. REC.1402.027 was used to perform this research at Shahrekord University of Medical Sciences. We thank the Shahrekord University of Medical Sciences Vice Chancellor for Study and Technology for their generous support of our study effort.

ABBREVIATION

TG: Thioguanine, MSN: Mesoporous Silica Nanoparticles, SF: Silk Fibroin, MCF-7: A breast cancer cell line, IC_{50}: Half Maximal Inhibitory Concentration, MTT: 3-(4,5-Dimethylthiazol-2-yl)-2,5-diphenyltetrazolium bromide, PI: Propidium Iodide, FBS: Fetal Bovine Serum, PBS: Phosphate-buffered saline, DMSO: Dimethyl Sulfoxide, G2/M: Gap 2/Mitosis phase in cell cycle, ATM: Ataxia Telangiectasia Mutated, ATR: ATM and Rad3-related, DDR: DNA Damage Response, Bax: BCL2 Associated X, Apoptosis Regulator, PUMA: p53 Upregulated Modulator of Apoptosis, CDK: Cyclin-Dependent Kinase, DOX: Doxorubicin, DOX-MSN-SS-CH-FA: Doxorubicin-loaded chitosan folate-capped dual-responsive Mesoporous Silica Nanoparticles, GNP: Gold Nanoparticles, MFI: mean Fluorescence Intensity, RGD: Arg-Gly-Asp (amino acid sequence), EDTA: Ethylenediaminetetraacetic Acid

AUTHORS CONTRIBUTIONS

Mohammad Amin Kaboli: data curation, writing original draft preparation, visualization, investigation. Javad Saffari-Chaleshtori: data curation, investigation, validation, supervision. Mehdi Rezaee: methodology, investigation, study design consultant. Sayedeh Azimeh Hosseini: laboratory test executive consultant, data curation, investigation. All authors have concurred that the descriptions are accurate and consistent, Pegah Khosravian. Finally, Dhiya Altememy and Alaa A. Hashim approved the publication.

CONFLICT OF INTERESTS

The authors declare no conflicts of interest.

REFERENCES

1. Giaquinto AN, Sung H, Miller KD, Kramer JL, Newman LA, Minihan A. Breast cancer statistics, 2022. CA Cancer J Clin. 2022;72(6):524-41. doi: 10.3322/caac.21754, PMID 36190501.
2. Gajbhiye SA, Patil MP. Solid lipid nanoparticles: a review on different techniques and approaches to treat breast cancer. Int J Appl Pharm. 2023;15(2):52-62.
3. Khoramdad M, Solaymani Dodaran M, Kabir A, Ghahremanzadeh N, Hashemi EO, Fahimfar N. Breast cancer risk factors in Iranian women: a systematic review and meta-analysis of matched case control studies. Eur J Med Res. 2022;27(1):311. doi: 10.1186/s40001-022-00952-0, PMID 36575538.
4. Kazeminia M, Salari N, Hosseinian Far A, Akbari H, Bazrafshan MR, Mohammadi M. The prevalence of breast cancer in Iranian women: a systematic review and meta-analysis. Indian J Gynecol Oncolog. 2022;20(1):14. doi: 10.1007/s40944-022-00613-4.
5. Youn HJ, Han W. A review of the epidemiology of breast cancer in Asia: focus on risk factors. Asian Pac J Cancer Prev. 2020;21(4):867-80. doi: 10.31557/APJCP.2020.21.4.867, PMID 32334446.
6. Cohen SY, Stoll CR, Anandarajah A, Doering M, Colditz GA. Modifiable risk factors in women at high risk of breast cancer: a systematic review. Breast Cancer Res. 2023;25(1):45. doi: 10.1186/s13058-023-01636-1, PMID 37095519.
7. Yang KN, Zhang CQ, Wang W, Wang PC, Zhou JP, Liang XJ. pH-responsive mesoporous silica nanoparticles employed in controlled drug delivery systems for cancer treatment. Cancer Biol Med. 2014;11(1):34-43. doi: 10.7497/j.issn.2095-3941.2014.01.003, PMID 24738037.
8. HO BN, Pfeffer CM, Singh AT. Update on nanotechnology-based drug delivery systems in cancer treatment. Anticancer Res. 2017;37(11):5975-81. doi: 10.21873/anticanres.12044, PMID 29061776.
9. Truong NP, Quinn JF, Whittaker MR, Davis TP. Polymeric filomicelles and nanoworms: two decades of synthesis and application. Polym Chem. 2016;7(26):4295-312. doi: 10.1039/C6PY00639F.
10. Jafari S, Derakhshankhah H, Alaei L, Fattahi A, Varnamkhasti BS, Saboury AA. Mesoporous silica nanoparticles for therapeutic/diagnostic applications. Biomed Pharmacother. 2019 Jan;109:1100-11. doi: 10.1016/j.biopha.2018.10.167, PMID 30551360.
11. Sharmiladevi S, Priya AS, Sujitha MV. Synthesis of mesoporous silica nanopaticles and drug loading for g-positive and g-negative bacteria. Int J Pharm Pharm Sci. 2016;8:196-201.
12. LI Z, Barnes JC, Bosoy A, Stoddart JF, Zink JI. Mesoporous silica nanoparticles in biomedical applications. Chem Soc Rev. 2012;41(7):2590-605. doi: 10.1039/c1cs15246g, PMID 22216418.
13. Bharti C, Nagaich U, Pal AK, Gulati N. Mesoporous silica nanoparticles in target drug delivery system: a review. Int J Pharm Investig. 2015;5(3):124-33. doi: 10.4103/2230-973X.160844, PMID 26258053.
14. Meijer B, Mulder CJ, Peters GJ, Van Bodegraven AA, DE Boer NK. Efficacy of thioguanine treatment in inflammatory bowel disease: a systematic review. World J Gastroenterol. 2016;22(40):9012-21. doi: 10.3748/wjg.v22.i40.9012, PMID 27833392.
15. Hashim AA, Abdul Reda Hussein U, Bahir H, Amir AA, Muhammad FA, Ahjel S. A DFT approach towards therapeutic potential of novel borospherene as targeted drug delivery system for isoniazid drug. Mol Phys. 2024;122(17):e2311786. doi: 10.1080/00268976.2024.2311786.
16. Zhang D, An X, LI Q, Man X, Chu M, LI H. Thioguanine induces apoptosis in triple-negative breast cancer by regulating PI3K–AKT pathway. Front Oncol. 2020;10:524922. doi: 10.3389/fonc.2020.524922, PMID 33194583.
17. Bayoumy AB, Simsek M, Seinen ML, Mulder CJ, Ansari A, Peters GJ. The continuous rediscovery and the benefit-risk ratio of thioguanine a comprehensive review. Expert Opin Drug Metab Toxicol. 2020;16(2):111-23. doi: 10.1080/17425255.2020.1719996, PMID 32090622.
18. Yamane K, Taylor K, Kinsella TJ. Mismatch repair mediated G2/M arrest by 6-thioguanine involves the ATR-Chk1 pathway. Biochem Biophys Res Commun. 2004;318(1):297-302. doi: 10.1016/j.bbrc.2004.04.030, PMID 15110787.
19. Cheng CP, Liu ST, Chiu YL, Huang SM, HO CL. The inhibitory effects of 6-thioguanine and 6-mercaptopurine on the USP2a target fatty acid synthase in human submaxillary carcinoma cells. Front Oncol. 2021;11:749661. doi: 10.3389/fonc.2021.749661, PMID 34956872.

20. Motasadizadeh H, Fatahi Y, Molla KV, Amanzadeh A, Farokhi M. New drug delivery systems based on polymeric silk fibroin. New Cell Mol Biotechnol J. 2019;9(34):9-22.
21. Panda N, Bissoyi A, Pramanik K, Biswas A. Development of novel electrospun nanofibrous scaffold from p. ricini and a. mylitta silk fibroin blend with improved surface and biological properties. Mater Sci Eng C Mater Biol Appl. 2015 Mar;48:521-32. doi: 10.1016/j.msec.2014.12.010, PMID 25579953.
22. Karimi Maleh H, Fallah Shojaei A, Karimi F, Tabatabaeian K, Shakeri S. Au nanoparticle loaded with 6-thioguanine anticancer drug as a new strategy for drug delivery. J Nanostruct. 2018;8(4):217-424. doi: 10.22052/JNS.2018.04.012.
23. Rajashekaraiah R, Kumar PR, Prakash N, Rao GS, Devi VR, Metta M. Anticancer efficacy of 6-thioguanine loaded chitosan nanoparticles with or without curcumin. Int J Biol Macromol. 2020 Apr 1;148:704-14. doi: 10.1016/j.ijbiomac.2020.01.117, PMID 31954127.
24. Cheema SK, Gobin AS, Rhea R, Lopez Berestein G, Newman RA, Mathur AB. Silk fibroin mediated delivery of liposomal emodin to breast cancer cells. Int J Pharm. 2007;341(1-2):221-9. doi: 10.1016/j.ijpharm.2007.03.043, PMID 17499461.
25. Gupta V, Aseh A, Rios CN, Aggarwal BB, Mathur AB. Fabrication and characterization of silk fibroin-derived curcumin nanoparticles for cancer therapy. Int J Nanomedicine. 2009;4:115-22. doi: 10.2147/ijn.s5581, PMID 19516890.
26. Mottaghitalab F, Farokhi M, Shokrgozar MA, Atyabi F, Hosseinkhani H. Silk fibroin nanoparticle as a novel drug delivery system. J Control Release. 2015;206:161-76. doi: 10.1016/j.jconrel.2015.03.020, PMID 25797561.
27. Ahmed A, Sarwar S, HU Y, Munir MU, Nisar MF, Ikram F. Surface modified polymeric nanoparticles for drug delivery to cancer cells. Expert Opin Drug Deliv. 2021;18(1):1-24. doi: 10.1080/17425247.2020.1822321, PMID 32905714.
28. Altememy D, Khoobi M, Javar HA, Alsamarrai S, Khosravian P. Synthesis and characterization of silk fibroin coated mesoporous silica nanoparticles for tioguanine targeting to leukemia. Int J Pharmacol Res. 2020;12(2):SP2.145. doi: 10.31838/ijpr/2020.
29. Comsa S, Cimpean AM, Raica M. The story of MCF-7 breast cancer cell line: 40 years of experience in research. Anticancer Res. 2015;35(6):3147-54. PMID 26026074.
30. Holliday DL, Speirs V. Choosing the right cell line for breast cancer research. Breast Cancer Res. 2011;13(4):215. doi: 10.1186/bcr2889, PMID 21884641.
31. Stockert JC, Horobin RW, Colombo LL, Blazquez Castro A. Tetrazolium salts and formazan products in cell biology: viability assessment fluorescence imaging and labeling perspectives. Acta Histochem. 2018;120(3):159-67. doi: 10.1016/j.acthis.2018.02.005, PMID 29496266.
32. Adan A, Kiraz Y, Baran Y. Cell proliferation and cytotoxicity assays. Curr Pharm Biotechnol. 2016;17(14):1213-21. doi: 10.2174/1389201017666160808160513, PMID 27604355.
33. Jiang L, Tixeira R, Caruso S, Atkin Smith GK, Baxter AA, Paone S. Monitoring the progression of cell death and the disassembly of dying cells by flow cytometry. Nat Protoc. 2016;11(4):655-63. doi: 10.1038/nprot.2016.028, PMID 26938116.
34. Crowley LC, Marfell BJ, Scott AP, Waterhouse NJ. Quantitation of apoptosis and necrosis by annexin v binding propidium iodide uptake and flow cytometry. Cold Spring Harb Protoc. 2016;2016(11):prot087288. doi: 10.1101/pdb.prot087288, PMID 27803250.
35. Hashim AA, Rajab NA, Tekie FS, Dinarvand R, Akrami M. Investigations factors affecting formulation of anastrozole as nanostructured lipid carrier. International Journal of Pharmaceutical Research. 2020;12(3):937-45. doi: 10.31838/ijpr/2020.
36. Yamane K, Taylor K, Kinsella TJ. Mismatch repair mediated G2/M arrest by 6-thioguanine involves the ATR–Chk1 pathway. Biochem Biophys Res Commun. 2004;318(1):297-302. doi: 10.1016/j.bbrc.2004.04.030, PMID 15110787.
37. Trudeau M, Charbonneau F, Gelmon K, Laing K, Latreille J, Mackey J. Selection of adjuvant chemotherapy for treatment of node positive breast cancer. Lancet Oncol. 2005;6(11):886-98. doi: 10.1016/S1470-2045(05)70424-1, PMID 16257797.
38. Vallet Regi M, Colilla M, Izquierdo Barba I, Manzano M. Mesoporous silica nanoparticles for drug delivery: current insights. Molecules. 2017;23(1):47. doi: 10.3390/molecules23010047, PMID 29295564.
39. Fritze A, Hens F, Kimpfler A, Schubert R, Peschka Suss R. Remote loading of doxorubicin into liposomes driven by a transmembrane phosphate gradient. Biochim Biophys Acta. 2006;1758(10):1633-40. doi: 10.1016/j.bbamem.2006.05.028, PMID 16887094.
40. Kumari A, Yadav SK, Yadav SC. Biodegradable polymeric nanoparticle-based based drug delivery systems. Colloids Surf B Biointerfaces. 2010;75(1):1-18. doi: 10.1016/j.colsurfb.2009.09.001, PMID 19782542.
41. Jafarizad A, Aghanejad A, Sevim M, Metin O, Barar J, Omidi Y. Gold nanoparticles and reduced graphene oxide gold nanoparticle composite materials as covalent drug delivery systems for breast cancer treatment. Chemistry Select. 2017;2(23):6663-72. doi: 10.1002/slct.201701178.
42. Meng H, Mai WX, Zhang H, Xue M, Xia T, Lin S. Codelivery of an optimal drug/siRNA combination using mesoporous silica nanoparticles to overcome drug resistance in breast cancer *in vitro* and *in vivo*. ACS Nano. 2013;7(2):994-1005. doi: 10.1021/nn3044066, PMID 23289892.
43. Bhavsar DB, Patel V, Sawant KK. Design and characterization of dual responsive mesoporous silica nanoparticles for breast cancer targeted therapy. Eur J Pharm Sci. 2020;152:105428. doi: 10.1016/j.ejps.2020.105428, PMID 32553643.
44. Aghevlian S, Yousefi R, Faghihi R, Abbaspour A, Niazi A, Jaberipour M. The improvement of anti-proliferation activity against breast cancer cell line of thioguanine by gold nanoparticles. Med Chem Res. 2013;22(1):303-11. doi: 10.1007/s00044-012-0030-1.
45. Deka SR, Singh R, Verma P, Kumar P. Design fabrication and evaluation of amphiphilic hyaluronic acid conjugates as efficient carriers of 6-thioguanine for *in vitro* anticancer drug delivery applications. Polym Int. 2023;72(2):205-16. doi: 10.1002/pi.6460.
46. LI H, An X, Zhang D, LI Q, Zhang N, YU H. Transcriptomics analysis of the tumor-inhibitory pathways of 6-thioguanine in MCF-7 cells via silencing DNMT1 activity. Onco Targets Ther. 2020;13:1211-23. doi: 10.2147/OTT.S236543, PMID 32103989.
47. Zhang YQ, Shen WD, Xiang RL, Zhuge LJ, Gao WJ, Wang WB. Formation of silk fibroin nanoparticles in water-miscible organic solvent and their characterization. J Nanopart Res. 2007;9(5):885-900. doi: 10.1007/s11051-006-9162-x.
48. Seib FP, Jones GT, Rnjak Kovacina J, Lin Y, Kaplan DL. PH-dependent anticancer drug release from silk nanoparticles. Adv Healthc Mater. 2013;2(12):1606-11. doi: 10.1002/adhm.201300034, PMID 23625825.
49. LI H, AN X, Zhang D, LI Q, Zhang N, YU H. Transcriptomics analysis of the tumor inhibitory pathways of 6-thioguanine in MCF-7 cells via silencing DNMT1 activity. Onco Targets Ther. 2020;13:1211-23. doi: 10.2147/OTT.S236543, PMID 32103989.
50. LI J, Wang Q, Xia G, Adilijiang N, LI Y, Hou Z. Recent advances in targeted drug delivery strategy for enhancing oncotherapy. Pharmaceutics. 2023;15(9):2233. doi: 10.3390/pharmaceutics15092233, PMID 37765202.
51. Wang X, Yang L, Chen ZG, Shin DM. Application of nanotechnology in cancer therapy and imaging. CA Cancer J Clin. 2008;58(2):97-110. doi: 10.3322/CA.2007.0003, PMID 18227410.
52. Zhao Y, Shen M, WU L, Yang H, Yao Y, Yang Q. Stromal cells in the tumor microenvironment: accomplices of tumor progression? Cell Death Dis. 2023;14(9):587. doi: 10.1038/s41419-023-06110-6, PMID 37666813.
53. Costa RL, Han HS, Gradishar WJ. Targeting the PI3K/AKT/mTOR pathway in triple-negative breast cancer: a review. Breast Cancer Res Treat. 2018;169(3):397-406. doi: 10.1007/s10549-018-4697-y, PMID 29417298.
54. Mac Cuaig WM, Samykutty A, Foote J, Luo W, Filatenkov A, LI M. Toxicity assessment of mesoporous silica nanoparticles upon intravenous injection in mice: implications for drug delivery. Pharmaceutics. 2022 Apr 30;14(5):969. doi: 10.3390/pharmaceutics14050969, PMID 35631554.
55. Liu Y, WU W, Cai C, Zhang H, Shen H, Han Y. Patient derived xenograft models in cancer therapy: technologies and applica-

tions. Signal Transduct Target Ther. 2023;8(1):160. doi: 10.1038/s41392-023-01419-2, PMID 37045827.

56. Soares S, Sousa J, Pais A, Vitorino C. Nanomedicine: principles properties and regulatory issues. Front Chem. 2018;6:360. doi: 10.3389/fchem.2018.00360, PMID 30177965.
57. Jaki T, Burdon A, Chen X, Mozgunov P, Zheng H, Baird R. Early phase clinical trials in oncology: realising the potential of seamless designs. Eur J Cancer. 2023;189:112916. doi: 10.1016/j.ejca.2023.05.005, PMID 37301716.
58. Oehler JB, Rajapaksha W, Albrecht H. Emerging applications of nanoparticles in the diagnosis and treatment of breast cancer. J Pers Med. 2024;14(7):723. doi: 10.3390/jpm14070723, PMID 39063977.
59. Younis MA, Tawfeek HM, Abdellatif AA, Abdel Aleem JA, Harashima H. Clinical translation of nanomedicines: challenges opportunities and keys. Adv Drug Deliv Rev. 2022 Feb;181:114083. doi: 10.1016/j.addr.2021.114083, PMID 34929251.